治療：HCC の画像診断にて、肝 S5 亜区域切除を実施した。

切除肝のマクロ像：

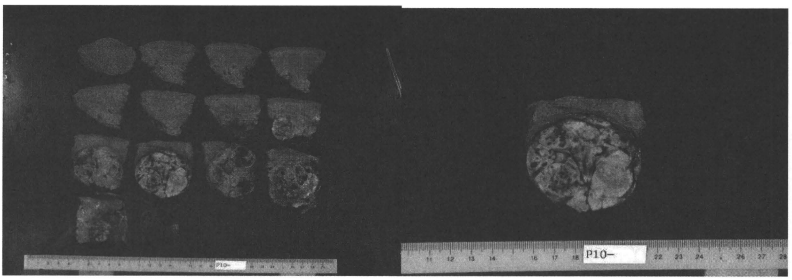

病理マクロ：結節型 HCC。結節内に種々の色調の小結節が含まれている。

VS(組織像)：

HCC の腫瘍細胞は肝細胞に類似し、索状に配列し、間質は内皮細胞より構成される類洞を形成する。(つまり、基本的にはその発生母体の肝臓を模倣した病理組織像を呈する)

HCC の腫瘍細胞の一般的所見：脂肪滴や糖原の沈着、細胞質内封入体（球状硝子体、Mallory 体、pale body)、胆汁産生などの所見がある。まず、他腫瘍との鑑別点として、腫瘍細胞には粘液はみられない。粘液産生が見られた場合には、胆管細胞癌、混合型肝癌、転移性腫瘍などを考慮する。

胆汁は肝細胞によってのみ産生される。従って、腫瘍に胆汁産生の所見が確認されれば HCC の診断が確定される。HCC における胆汁は、腫瘍細胞の胞体内、毛細胆管内、あるいは偽腺腔内に褐色調の小顆粒物質、あるいは胆汁栓などの形で存在する。胆汁産生は、比較的分化度の高い HCC に見られる傾向がある。

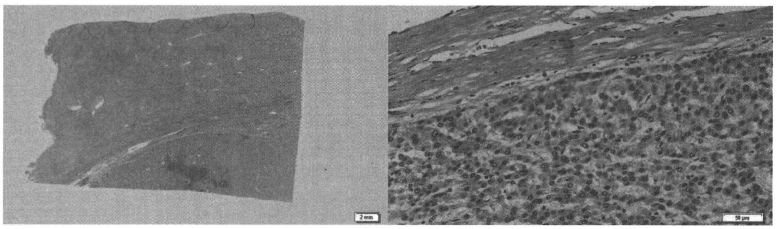

結節型 HCC で線維性被膜がみられる。

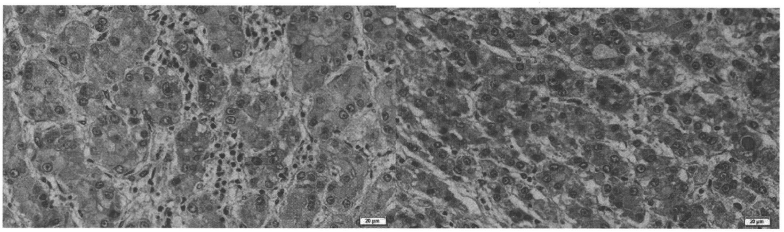

VS(HE): HCC 細胞のマロリー体　　VS(HE): HCC 細胞の胆汁栓

肝臓の解剖、組織像など

肝臓の正常組織像：

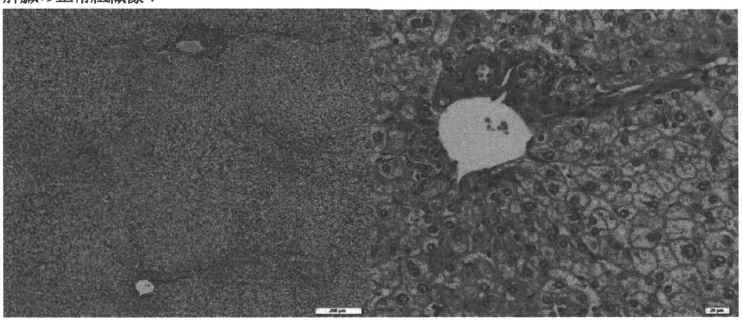

C. 研究結果

(1) 各種画像をシームレスに見る方法により、それらの対応が容易になり、画像カンファランスに際して画像所見の読みを深めるのに有用であった。また、臨床医・病理医間の症例検討の際にも非常に有用であった。

(2) 肝疾患を対象にした学習ツールでは、各種の情報に迅速にアクセスできるので、疾患を総合的に効率よく学習することが可能となった。

D. 考察

臨床医は治療法の選択、予後の推測などに役立つ病理診断情報を求めており、臨床医が読みもしない冗長で退屈な記載、形態分野に閉じこもった病理形態情報の枠内での従来の学習では不十分である。今回の研究でCT・MRIなどの放射線科で扱う画像と病理マクロ・ミクロ画像をシームレスに観察できる病理検索法を示したが、臨床画像の成り立ちの理解を促進するのに有用と思われる。さらに各種臨床情報とも容易に関連づけるツールを目指しているが、重要なことは各種情報の羅列ではなく、それらの関連性をより深いレベルで考察できる、あるいはそれを促すツール内容であるかが問われている。米国Digital Pathology Associationの学術集会“Pathology Visions 2010”での会長の基調講演でも統合的で、診断・治療・予後など臨床医の求める情報を組み込んだ病理診断報告書の追求が述べられたが、この方向性は今回の学習ツールのあり方、病理診断のあり方を示していると思われる。

今回の学習ツールを利用する際に、各疾患の記載内容がコンパクトで使いやすいことが重要である。より詳細な内容を学習したい人の為に、多分野の情報を含む「ライブラリー」にリンクして学習の理解を深める仕組みも有用と思われる。

E. 結論

疾患を総合的に学習できるツールの開発により、医師教育を促進し、医療の質向上が期待される。

F. 健康危険情報

特になし。

G. 研究発表

1.論文発表

1) Hiraoka A, Ochi H, Hidaka S, Uehara T, Hasebe A, Tanihira T, Miyamoto Y, Ninomiya T, Kawasaki H, Sogabe I, Ishimaru Y, Miyagawa M, Furuya K, Hirooka M, Abe M, Hiasa Y, Matsuura B, Onji M, Michitaka K:

FDG positoron emission tomography/computed tomography findings for the predection of early recurrence of hetatocellular carcinoma ater surgical resection. Experimental and Therapeutic Medicine. 1: 829-32(2010)

2) Muramori K, Taguchi S, Taguchi T, Kohashi K, Furuya K, Tokuda K, Ishii E: High aromatase activity and overexpression of epidermal growth factor receptor in fibrolamellar hepatocellular carcinoma in achild. J Pedriatr Hematol Oncol. (in press)

3) Kan M, Hiraoka A, Uehara T, Hidaka S, Ichiryu M, Nakahara H, Ochi H, Tanabe A, Kodama A, Hasebe A, Miyamoto Y, NinomiyaT, Abe M, Hiasa Y, Matsumura B, Onji M, Shinbata Y, Kameoka C, Doi S, Tamura H, Furuya K, Michitaka K: Evaluation of contrast-enhanced ultrasonography using perfluorobutane (Sonazoid) in patients with small hepatocellular carcinoma: Comparison with dynamic computed tomography. Oncology Letters. 1: 485-488(2010)

4) Ohtsuki Y, Maeda T, Soga Y, Furuya K, Okada Y, Lee G, Furihata M: Case report: Immunohistochemical characterization of pulmonary corpora amylacea in an autopsy case, with special reference to its pathogenesis. Biomedical Res. 21(3): 230-232(2010)

H. 知的財産権の出願・登録状況

1. 特許取得
   なし
2. 実用新案登録
   なし
3. その他

なし

FDG positron emission tomography/computed tomography findings for the prediction of early recurrence of hepatocellular carcinoma after surgical resection

ATSUSHI HIRAOKA[1], HIRONORI OCHI[1], SATOSHI HIDAKA[1], TAKAHIDE UEHARA[1], AKI HASEBE[1], TETSUYA TANIHIRA[1], YASUNAO MIYAMOTO[1], TOMOYUKI NINOMIYA[1], HIDEKI KAWASAKI[2], ICHIRO SOGABE[3], YOSHIHIRO ISHIMARU[3], MASAO MIYAGAWA[3], KEIZO FURUYA[4], MASASHI HIROOKA[5], MASANORI ABE[5], YOICHI HIASA[5], BUNZO MATSUURA[5], MORIKAZU ONJI[5] and KOJIRO MICHITAKA[1]

[1]Gastroenterology Center; Departments of [2]Surgery, [3]Radiology, and [4]Pathology, Ehime Prefectural Central Hospital; [5]Department of Gastroenterology and Metabology, Ehime University Graduate School of Medicine, Ehime, Japan

Received May 13, 2010; Accepted June 29, 2010

DOI: 10.3892/etm.2010.126

Abstract. We investigated the predictive value of fluorine-18-fluorodenoxyglucose positron emission tomography/computed tomography for pathological malignant potential and early recurrence of hepatocellular carcinoma (HCC) after resection. From April 2006 to October 2009, 53 patients with naïve HCC were enrolled. Accumulations of 2-[18F]-fluoro-2-deoxy-D-glucose (FDG) standardized uptake value (SUVmax) in both HCC and non-HCC areas of the liver as well as the ratio of SUVmax (R-SUV; HCC/liver) were calculated. The results were evaluated to determine prognostic factors for early recurrence. One patient was graded as tumor node metastasis stage I, 35 as II, 14 as III and 3 as stage IV. Elevated protein induced by vitamin K absence or antagonist II (≥200 mAU/ml) as well as elevated fucosylated α-fetoprotein (≥15%), tumor size (≥5 cm) and high R-SUV (≥1.5) were risk factors for early recurrence in a univariate analysis (P<0.05). In a multivariate analysis, high R-SUV (≥1.5) was the only risk factor (P<0.05). The recurrence-free rate in patients with low R-SUV (<1.5, n=34) was higher than that in those with high R-SUV (≥1.5, n=19) (1- and 2-year rates: 100 and 67%, 67 and 17%; respectively, P<0.01). Patients with Edmondson III showed higher R-SUV values than those with Edmondson I and II (3.0±1.8, 1.4±0.3 and 1.9±0.9, respectively, P<0.01), while those with micro-vascular invasion (vp)(+), micro-intrahepatic metastasis (im)(+) or non-boundary type showed higher R-SUV values than vp(-), im(-) and boundary type (3.6±2.4 vs. 2.0±0.9, 3.5±2.3 vs. 1.9±0.8 and 2.9±1.8 vs. 1.6±0.5, respectively, P<0.01). R-SUV is proposed to be a useful marker for the prediction of early recurrence of HCC after resection.

Correspondence to: Atsushi Hiraoka, Gastroenterology Center, Ehime Prefectural Central Hospital, Kasuga-Cho 83, Matsuyama, Ehime 790-0024, Japan
E-mail: hirage@m.ehime-u.ac.jp

Key words: 2-[18F]-fluoro-2-deoxy-D-glucose, positron emission tomography, computed tomography, hepatocellular carcinoma, prognosis, hepatic resection, recurrence

Introduction

Recently, 2-[18F]-fluoro-2-deoxy-D-glucose (FDG) positron emission tomography (PET)/computed tomography (CT) has been used for diagnosing malignant tumors, and many reports have described its role for predicting the malignant potential of these tumors. However, the clinical efficacy of PET/CT for diagnosing hepatocellular carcinoma (HCC) remains controversial, and only a few reports have described the predictive value of its findings for pathological malignant potential and prognosis (1-3).

Hepatic resection is performed as a standard therapy for HCC in Japan (4,5). However, recurrence of HCC after resection is known to occur at a high rate, and early recurrence is considered to be a significant prognostic factor for death. Although macroinvasion of HCC to the portal vein is also a factor for poor prognosis (6), most patients with HCC without macro-tumor thrombosis suffer from recurrence after resection. Previous reports have investigated prognostic markers for early recurrence and survival, including the doubling time of pre-operative serum α-fetoprotein (AFP) and protein induced by vitamin K absence or antagonist II (PIVKA-II) (7), complication with diabetes mellitus (8), hepatic steatosis (9) and tumor node metastasis (TNM) stage (10), although these are not adequately sensitive. In the present study, we investigated the predictive value of PET/CT for the pathological malignant potential of HCC as a new indicator for early recurrence after hepatic resection.

Materials and methods

From April 2006 to October 2009, 53 patients with naïve HCC, examined by PET/CT and treated by hepatic resection, were enrolled. None had poorly controlled diabetes mellitus. All were examined using PET/CT (Discovery ST Elite 16; GE Healthcare Japan Co. Ltd., Tokyo, Japan) within the month

Table I. Univariate analysis of clinical parameters for early recurrence after resection.

Factors	No.	Hazard ratio	95% CI	P-value
Age in years (<70:≥70)	23:30	0.662	0.234-1.873	0.437
Anti-HCV (positive:negative)	28:25	0.612	0.221-1.674	0.345
Gender (male:female)	40:13	0.688	0.189-2.507	0.571
Aspartate transferase (IU/l) (<80:≥80)	44:9	2.501	0.841-7.437	0.099
Alanine transferase (IU/l) (<80:≥80)	48:5	3.710	0.956-14.402	0.058
Total bilirubin (mg/dl) (<2:≥2)	52:1	0.048	0.000-2.823	0.810
Albumin (g/dl) (<3.5:≥3.5)	11:42	1.456	0.307-6.904	0.636
Prothrombin time (%) (<80:≥80)	25:28	0.923	0.341-2.493	0.874
Platelets (x10^4 cells/μl) (<12:≥12)	18:35	1.453	0.515-4.098	0.480
Child-Pugh (A:B)	44:9	1.679	0.352-8.003	0.515
AFP (ng/ml) (<100:≥100)	41:12	1.996	0.619-6.441	0.248
AFP-L3 (%) (<15:≥15)	38:15	3.165	1.101-9.095	0.032
PIVKA-II (mAU/ml) (<200:≥200)	31:22	3.805	1.285-11.267	0.016
Diabetes mellitus (positive:negative)	16:37	0.371	0.102-1.354	0.133
No. of HCC (multiple:single)	15:38	1.578	0.540-4.607	0.404
Tumor size (<5 cm:≥5 cm)	31:22	3.050	1.036-8.983	0.043
R-SUV (<1.5:≥1.5)	19:34	10.581	1.394-80.343	0.023

CI, confidence interval; HCV, hepatitis C virus; AFP, α-fetoprotein; AFP-L3, fucosylated AFP; PIVKA-II, protein induced by vitamin K absence or antagonist II; TNM stage, tumor node metastasis stage; R-SUV, ratio of accumulations of FDG in HCC and non-HCC areas of the liver.

prior to resection. PET/CT was performed 60 min after a bolus injection of F-18 FDG (3 MBGq/kg). Accumulations of FDG [standardized uptake value (SUVmax)] in HCC and non-HCC areas of the liver as well as the ratio of SUVmax (R-SUV), which indicated the tumor to non-tumor ratio, were determined. In cases with multiple HCC, the SUVmax was calculated for the main nodule. From these findings, we evaluated prognostic factors for early recurrence, which was defined as recurrence within 2 years of resection. Moreover, R-SUV values were compared to the pathological findings, including microvascular invasion (vp), micro-intrahepatic metastasis (im) and gross type of HCC (11,12). The patients were divided into two groups, low R-SUV (n=19) and high R-SUV (n=34), and their clinical parameters were compared.

Statistical analysis. Data are expressed as the mean ± standard deviation (SD). Statistical analyses were performed using the Student's t-test for unpaired data, a χ^2 test, Fischer's exact test, a Mann-Whitney U test and a log-rank test, as appropriate. All statistical analyses were performed with SPSS 16.0J (SPSS Japan Inc., Tokyo, Japan). A P-value of <0.05 was considered to represent statistical significance.

Results

One patient was classified as TNM stage I, 35 as stage II, 14 as stage III and 3 as stage IV, based on the results of imaging examinations (abdominal ultrasonography and dynamic CT). There were no cases with extrahepatic metastasis. R-SUV values ranged from 1.0 to 6.9. In pathological analyses, all were diagnosed as typical HCC. PIVKA-II (≥200 mAU/ml), fucosylated AFP (AFP-L3) (≥15%), tumor size (≥5 cm) and high R-SUV (≥1.5) were found to be risk factors for early recurrence in a univariate analysis (P<0.05, respectively) (Table I). In a multivariate analysis, high R-SUV (≥1.5) was the only risk factor (P<0.05) (Table II). The recurrence-free rate in the low R-SUV group was higher than that in the high R-SUV group (1- and 2-year recurrence-free rates: 100 and 67%, 67 and 17%, respectively; P<0.01) (Fig. 1). While the frequencies of high levels of PIVKA-II (≥200 mAU/ml) and AFP-L3 (≥15%) were greater in the high R-SUV group (52.9 and 38.2% vs. 21.1 and 10.5%, respectively; P<0.01), there were no significant differences in regard to the frequencies of high levels of AFP (≥100 ng/ml), tumor diameter ≥5 cm, Child-Pugh class, number of tumors and TNM stage between the groups (Table III).

Table II. Multivariate analysis of clinical parameters for early recurrence after resection.

Factors	Hazard ratio	95% CI	P-value
AFP-L3 (≥15%)	1.644	0.510-5.308	0.405
PIVKA-II (≥200 mAU/ml)	2.113	0.481-9.275	0.322
Tumor size (≥5 cm)	1.157	0.271-4.935	0.843
R-SUV (≥1.5)	8.137	1.027-64.466	0.047

CI, confidence interval; AFP-L3, fucosylated α-fetoprotein; PIVKA-II, protein induced by vitamin K absence or antagonist II; R-SUV, ratio of accumulations of FDG in HCC and non-HCC areas of the liver.

Patients with HCC nodules rated as Edmondson III (13) had a higher R-SUV value (3.0±1.8) than those rated as I

Table III. Clinical background of the patients.

	Low R-SUV group (n=19)	High R-SUV group (n=34)	P-value
Age (years)	68.2±14.1	69.5±10.5	0.705
Anti-HCV (positive:negative)	13:6	15:19	0.092
Gender (male:female)	15:4	25:9	0.705
Aspartate transferase (IU/l)	49.4±32.2	50.2±25.8	0.308
Alanine transferase (IU/l)	40.5±25.4	41.5±27.8	0.934
Total bilirubin (mg/dl)	0.79±0.49	0.66±0.28	0.085
Albumin (g/dl)	4.0±0.6	4.0±0.5	0.555
Prothrombin time (%)	80.1±12.2	81.2±9.9	0.127
Platelets ($x10^4$ cells/μl)	13.0±4.7	16.0±5.7	0.696
Child-Pugh class (A:B)	15:4	29:5	0.528
AFP (ng/ml)	371.2±1,199.4	2,306.5±12,657.9	0.201
AFP-L3 (%)	1.6±5.1	16.9±23.9	<0.001
PIVKA-II (mAU/ml)	424.4±1,123.6	8,436.2±17,683.6	0.001
Tumor size (<5 cm:≥5 cm)	14:5	17:17	0.077
No. of tumors	1.4±0.7	1.4±0.7	0.819
Score of up to 7 criteria	5.0±1.7	7.4±3.4	0.013
TNM stage (I:II:III:IV)	1:13:5:0	0:22:9:3	0.320
Mean R-SUV	1.23±1.45	2.73±1.65	<0.001

HCV, hepatitis C virus; AFP, α-fetoprotein; AFP-L3, fucosylated AFP; PIVKA-II, protein induced by vitamin K absence or antagonist II; TNM stage, tumor node metastasis stage; R-SUV, ratio of accumulations of FDG in HCC and non-HCC areas of the liver.

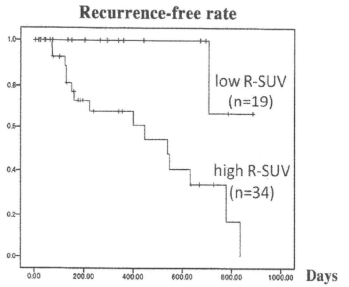

Figure 1. Recurrence rates in both patient groups. A higher level of early recurrence after resection was observed in the high R-SUV group (P<0.01).

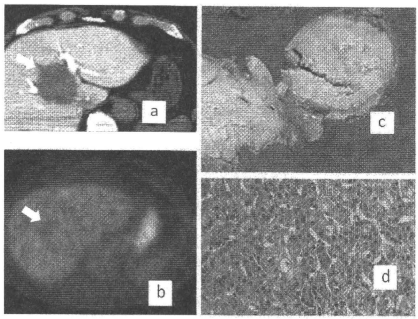

Figure 2. Accumulations of FDG (SUV) in both the HCC and non-HCC areas of the liver. The ratio (R-SUV) was calculated using FDG PET/CT findings. Representative case with HCC in the 4th segment of the liver (5.1 cm in diameter). (a) The tumor is observable as a defect in the CT arterial portography findings. (b) A low R-SUV value (1.4) was revealed by FDG PET/CT. (c) Resected specimen showing the tumor as a single nodular type. (d) The tumor was diagnosed as a well-differentiated HCC (Edmondson I) from the histological findings.

and II (1.4±0.3 and 1.9±0.9, respectively; P<0.01). Patients with nodules showing vp(+) and im(+), and with non-boundary type of nodules (single nodular type with extranodular growth, confluent multinodular or invasive type) had higher R-SUV values than those with vp(-), im(-) or boundary type (vaguely nodular or single nodular type) (3.6±2.4 vs. 2.0±0.9, 3.5±2.3 vs. 1.9±0.8 and 2.9±1.8 vs. 1.6±0.5, respectively; P<0.01). Throughout the observation period, extrahepatic metastasis was observed in 2 cases of stage II; these cases had high R-SUV (2.3 and 2.4, respectively). Fig. 2 shows representative results of a patient with low R-SUV (1.4) whose pathological findings were single nodular type, Edmondson I, and who was negative for both vp and im. By contrast, Fig. 3 presents the results of a representative patient with high R-SUV (1.9) whose pathological findings were confluent multinodular type, Edmondson III and positive for vp, though the tumor size was small (2.5 cm in diameter).

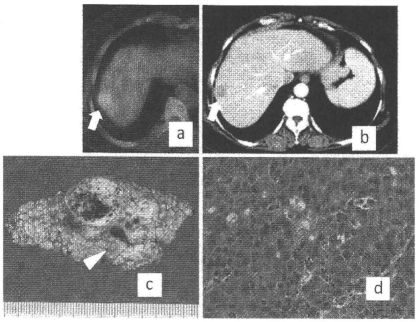

Figure 3. Representative case with HCC in the 8th segment of the liver (2.5 cm in diameter). (a) The tumor is noted as a defect in the CT arterial portography findings. (b) The tumor had a high R-SUV value (1.9) as shown by FDG PET/CT. (c) Resected specimen showing the tumor as a confluent multinodular type with macroinvasion to the 8th portal vein (arrowhead). Invasion of the portal vein was not detected in an imaging examination conducted 2 weeks before surgical resection. (d) The tumor was diagnosed as a poorly differentiated HCC (Edmondson III) upon histological examination.

Discussion

In Japan, the shortage of donors for liver transplantation is a major obstacle to the treatment of HCC, thus hepatic resection is often performed as curative therapy (4,5). FDG-PET/CT is a functional imaging modality that is used to measure the glucose metabolism of malignant tumors, although its clinical efficacy has not been established. The ability of PET to detect HCC in the liver was found to be less effective than that of contrast enhanced CT (14). On the other hand, Yoon *et al* (15) and Sugiyama *et al* (16) reported that PET is useful for the screening of extrahepatic metastasis from HCC. Recently, the usefulness of FDG-PET for predicting HCC recurrence following liver transplantation was proposed (17,18). However, few reports have described FDG-PET as useful for predicting prognosis after resection (1,2). Kawamura *et al* found that even in patients diagnosed in the early phase of HCC, a high R-SUV value among other prognostic scores may indicate poor prognosis or the need for radical treatment (3). The present results are similar to past reports, which showed that a high R-SUV value is capable of predicting early recurrence after resection, and that the relationship between a high R-SUV and pathological malignant potential is associated with positive findings for im or vp (19), higher Edmondson grade and worse gross type (11,12) in resected specimens. Since the average R-SUV of Edmondson I was <1.5, we set 1.5 as the cut off; this cut off value predicted the early recurrence of HCC.

Full body scanning with PET/CT is useful for the screening of extrahepatic metastasis and staging in patients with large HCC (15). An FDG-PET/CT examination is non-invasive and useful for predicting the malignant pathological potential of HCC before resection without the need for a biopsy. However, patients with high R-SUV values must be followed carefully with imaging modalities after resection.

In conclusion, we found that HCC patients with a high R-SUV value (≥1.5) had an elevated risk of early recurrence after resection, while R-SUV was also shown to be related with pathological findings. Thus, R-SUV is proposed as a useful predictive marker for the early recurrence of HCC before surgical resection.

References

1. Shiomi S, Nishiguchi S, Ishizu H, *et al*: Usefulness of positron emission tomography with fluorine-18-fluorodenoxyglucose for predicting outcome in patients with hepatocellular carcinoma. Am J Gastroenterol 96: 1877-1880, 2001.
2. Hatano E, Ikai I, Higashi T, *et al*: Preoperative positron emission tomography with fluorine-18-fluorodeoxyglucose in predictive of prognosis in patients with hepatocellular carcinoma after resection. World J Surg 30: 1736-1741, 2006.
3. Kawamura E, Habu D, Ohfuji S, *et al*: Clinical role of FDG-PET for HCC: relationship of glucose metabolic indicator to Japan Integrated Staging (JIS) score. Hepatogastroenterology 55: 582-586, 2008.
4. Arii S, Yamaoka Y, Futagawa S, *et al*: Results of surgical and nonsurgical treatment for small-sized hepatocellular carcinomas: a retrospective and nationwide survey in Japan. The Liver Cancer Study Group of Japan. Hepatology 32: 1224-1229, 2000.
5. Ikai I, Arii S, Kojiro M, *et al*: Reevaluation of prognostic factors for survival after liver resection in patients with hepatocellular carcinoma in a Japanese nationwide survey. Cancer 101: 796-802, 2004.
6. Arii S, Tanaka J, Yamazoe Y, *et al*: Predictive factors for intrahepatic recurrence of hepatocellular carcinoma after partial hepatectomy. Cancer 69: 913-919, 1992.
7. Masuda T, Beppu T, Horino K, *et al*: Preoperative tumor marker doubling time is a useful predictor of recurrence and prognosis after hepatic resection of hepatocellular carcinoma. J Surg Oncol: Nov, 24, 2009 (E-pub ahead of print).
8. Komura T, Mizukoshi E, Kita Y, *et al*: Impact of diabetes on recurrence of hepatocellular carcinoma after surgical treatment in patients with viral hepatitis. Am J Gastroenterol 102: 1939-1946, 2007.
9. Takuma Y, Nouso K, Makino Y, *et al*: Hepatic steatosis correlates with the postoperative recurrence of hepatitis C virus-associated hepatocellular carcinoma. Liver Int 27: 620-626, 2007.
10. Poon RT, Ng IO, Fan ST, *et al*: Clinicopathologic features of long-term survivors and disease-free survivors after resection of hepatocellular carcinoma: a study of a prospective cohort. J Clin Oncol 19: 3037-3044, 2001.
11. Stroffolini T, Andreone P, Andriulli A, *et al*: Gross pathologic types of hepatocellular carcinoma in Italy. Oncology 56: 189-192, 1999.
12. Iguchi T, Aishima S, Sanefuji K, *et al*: Both fibrous capsule formation and extracapsular penetration are powerful predictors of poor survival in human hepatocellular carcinoma: a histological assessment of 365 patients in Japan. Ann Surg Oncol 16: 2539-2546, 2009.
13. Edmondson HA and Steiner PE: Primary carcinoma of the liver. A study of 100 cases among 48900 necrosis necropsies. Cancer 7: 462-503, 1954.
14. Trojan J, Schroeder O, Raedle J, *et al*: Fluorine-18 FDG positron emission tomography for imaging of hepatocellular carcinoma. Am J Gastroenterol 94: 3314-3319, 1999.
15. Yoon KT, Kim JK, Kim DY, *et al*: Role of 18F-fluorodeoxyglucose positron emission tomography in detecting extrahepatic metastasis in pretreatment staging of hepatocellular carcinoma. Oncology 72: 104-110, 2007.
16. Sugiyama M, Sakahara H, Torizuka T, *et al*: 18F-FDG PET in the detection of extrahepatic metastases from hepatocellular carcinoma. J Gastroenterol 39: 961-968, 2004.
17. Lee JW, Paeng JC, Kang KW, *et al*: Prediction of tumor recurrence by 18F-FDG PET in liver transplantation for hepatocellular carcinoma. J Nucl Med 50: 682-687, 2009.
18. Komberg A, Freesmeyer M, Barthel E, *et al*: 18F-FDG-uptake of hepatocellular carcinoma on PET predicts microvascular tumor invasion in liver transplant patients. Am J Transplant 9: 592-600, 2009.
19. Sumie S, Kuromatsu R, Okuda K, *et al*: Microvascular invasion in patients with hepatocellular carcinoma and its predictable clinicopathological factors. Ann Surg Oncol 15: 1375-1382, 2008.

CE: Ramya ED: Mng Op: Balu MPH:201313

High Aromatase Activity and Overexpression of Epidermal Growth Factor Receptor in Fibrolamellar Hepatocellular Carcinoma in a Child

Katsumi Muramori, MD, PhD, Syouhei Taguchi, MD, PhD,* Tomoaki Taguchi, MD, PhD,† Kenichi Kohashi, MD, PhD,‡ Keizo Furuya, MD, PhD,§ Kiriko Tokuda, MD,‖ and Eiichi Ishii, MD, PhD¶*

Summary: An 11-year-old boy was admitted with a liver tumor and underwent right trisegmentectomy for a diagnosis of fibrolamellar hepatocellular carcinoma. He had suffered from bilateral gynecomastia for a year, which improved after complete resection of the tumor. The tumor cells had significant aromatase activity (8.03 pmol/g/h) and contained high levels of estradiol (82.1 pg/mL), which contributed to gynecomastia. Furthermore, overexpression of epidermal growth factor receptor was determined in the tumor cells, which suggests that antitumor strategies using epidermal growth factor receptor antagonists may be effective.

Key Words: fibrolamellar hepatocellular carcinoma, gynecomastia, aromatase, epidermal growth factor receptor

(*J Pediatr Hematol Oncol* 2010;00:000–000)

Fibrolamellar hepatocellular carcinoma (FL-HCC) is a rare liver tumor which arises most often in young adults.[1–3] Effective therapies other than surgical resection, including liver transplantation, have not been reported.[1,4,5] In fact, recent studies have noted that prognosis is as poor as in conventional hepatocellular carcinoma (HCC) arising in a noncirrhotic liver.[6] The effectiveness of chemotherapy against solid tumors has in general been limited, but molecular targeting therapies are being developed. One of these strategies, which uses antagonists of the epidermal growth factor receptor (EGFR) family, has recently been used. EGFR is known to be overexpressed not only by epithelial tumors[7] but also by conventional HCC.[8] In contrast, gynecomastia in children has been reported to be a sign of FL-HCC and was exacerbated by aromatase activity in the tumor cells.[9–11]

CASE REPORT

A prepubertal 11-year-old boy had been followed for bilateral gynecomastia for 1 year at the hospital and was finally admitted for fever and headache. Initially, meningitis was suspected. However C-reactive protein levels were persistently elevated, despite the decline in his fever induced by administration of antibiotics. Subsequently, a gallium scintigraphic study revealed positive scintigraphic accumulation at the right lobe of the liver. He was then referred to our hospital for tumor evaluation. Computed tomographic examination revealed a liver mass 12 cm in diameter with a central scar accompanied by calcification (Fig. 1).[12] Fluorodeoxyglucose positron emission tomography examination was negative. Only one tumor marker, PIVKA II, was slightly elevated at 64 mAU/mL (range < 40); but α-fetoprotein (0.5 ng/mL) was within normal range. Serum examination for gynecomastia revealed high estradiol levels of 23.0 pg/mL (prepubertal range < 10 pg/mL), as well as low luteinizing hormone (LH) < 0.1 mIU/mL (range: 0.6 to 4.1 mIU/mL) and follicle-stimulating hormone (FSH) levels < 0.1 mIU/mL (range: 2.9 to 10.2 mIU/mL), which were

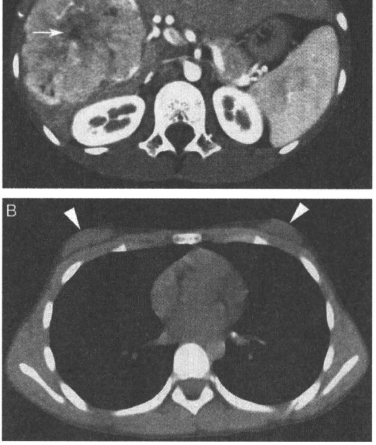

FIGURE 1. Contrast-enhanced abdominal computed tomographic scan showing a large heterogeneous mass about 12 cm in diameter with a central scar occupying the right lobe.

Received for publication March 29, 2010; accepted October 11, 2010.
From the *Departments of *Pediatric Surgery; §Pathology; ‖Pediatrics, Ehime Prefectural Central Hospital, Matsuyama; †Departments of †Pediatric Surgery; ‡Anatomic Pathology, University of Kyushu, Fukuoka; and ¶Department of Pediatrics, University of Ehime, Ehime, Japan.

Reprints: Katsumi Muramori, MD, PhD, Department of Pediatric Surgery, Ehime Prefectural Central Hospital, 83 Kasuga-machi, Matsuyama 790-0024, Japan (e-mail: c-kmuramori@eph.pref.ehime.jp).

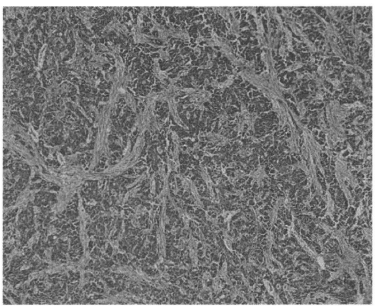

FIGURE 2. A photomicrograph (hematoxylin eosin stain) of the resected tumor demonstrates that the tumor consists of large polygonal cells with abundant eosinophilic cytoplasm, large vesiculated nuclei, and large nucleoli, with lamellar fibrosis.

suspicious for negative feedback from gonadotropin. The tumor was resected by right hepatectomy (Couinaud nomenclature: S5 to S8) with lymph node dissection in the hepatoduodenal ligament, and pathologic evaluation returned a FL-HCC without lymph node metastasis (Fig. 2). Immunohistochemical staining with the EGFR pharmDx kit (Dako Japan, Inc, Kyoto, Japan) showed strong membrane expression in tumor cells (Fig. 3). No activating mutation in exon2 of the *k-ras* gene was detected. The presence of other activating mutations such as G719S/C/A (exon18), E746-A750del (2types) and L747-P753delinsS (exon19), S768I (exon20), L858R, and L861Q (exon21) were not determined by polymerase chain reaction-invader assay which was carried out at Bio Medical Laboratories (Japan). Intratumor aromatase activity was measured by tritium release water assay and intratumor estradiol concentration was measured by liquid chromatography: tandem mass spectrometry at the laboratory of ASKA Pharma edical Co, Ltd, Japan. Estradiol concentration and aromatase activity in the tumor cells were 82.1 pg/mL and 8.03 pmol/g/h, respectively. The patient's gynecomastia gradually improved after the operation, whereas serum estradiol became undetectable, and LH and FSH returned to normal levels (Table 1). The patient received 3 sets of chemotherapy with cisplatin and 4′-0-tetrahydropyranyladriamycin hydrochloride before discharge according to Japanese Study Group for Pediatric Liver Tumor 2 protocol, and no recurrence was detected for 15 months.

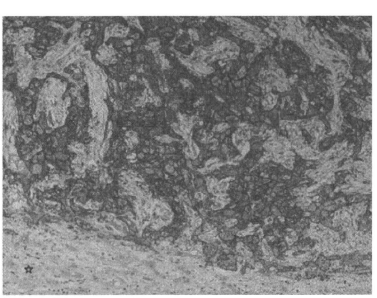

FIGURE 3. Immunochemical staining for EGFR showing overexpression in tumor cells. Normal liver cells were not stained (☆).

TABLE 1. Levels of Hormones Related to Gynecomastia

	Preoperative	Postoperative (2 wk After Resection)
Estradiol (pg/mL)	23.0	< 5.0
Testosterone (ng/dL)	39.4	21.0
LH (mIU/mL)	< 0.1	0.5
FSH (mIU/mL)	< 0.1	4.7

Serum estradiol rapidly declined to undetectable levels after complete resection of the liver tumor.
FSH indicates follicle-stimulating hormone; LH, luteinizing hormone.

DISCUSSION

Compared with its prevalence, FL-HCC is a rare HCC which more often affects young adults without cirrhotic liver. Rational prevalence was reported in Whites, but the disease is very rare in Asians and Africans.[1] The Liver Cancer Study Group of Japan reported that the number of FL-HCC cases registered had increased to 0.68% of all reported HCC cases (2002 to 2003) and that in children, FL-HCC was still extremely rare. Although its clinical characteristics are well documented,[1] unusual presentations for FL-HCC have also been reported.[1,10,11,13] Among the symptoms reported, gynecomastia was characteristically present (Table 2), and high aromatase activity in the tumor cells contributed to production of estrogen, resulting in bilateral gynecomastia[10,11]; this was also proven on a molecular level.[9] Aromatase is a steroid-type enzyme that converts C_{19} steroids to esterone and estradiol in many kinds of human cells. Aromatase expression is controlled by tissue-specific promoters, and high expression in fetal liver cells has also been reported; however, this disappears in the postnatal period.[9] In our case, it was clear that activation of aromatase by the tumor cells significantly contributed to the gynecomastia by producing estrogen in the tumor cells. Consequently, serum estradiol levels rapidly decreased, and suppression of LH and FSH halted after resection of the tumor (Table 1).

On the other hand, EGFR is a member of the tyrosine kinase receptor family and is encoded by the *c-erb*B oncogenes. Its activation leads to stimulation of nuclear transcription and cellular proliferation via the ras/raf, protein kinase C and phosphatidylinositol-3-kinase pathways.[7] EGFR has been associated with tumor proliferation, and its presence in epithelial tumors has been documented as follows: 40% to 80% of nonsmall cell lung cancers, 25% to 77% of colorectal cancers, 40% of prostate cancers, 35% to 70% of ovarian cancers, 33% of advanced gastric cancers, 30% to 50% of pancreatic cancers, 15% to 30% of breast cancers, and 50% of bladder cancers[7]; in addition, its overexpression in some of these tumors has been associated with poor prognosis.[15] Although EGFR remains a controversial prognostic factor in some cancers,[16] a trend toward poor prognosis was also found in conventional HCC and FL-HCC.[8] Overexpression of EGFR was observed in 40% to 70% of HCCs[8] and in a majority of FL-HCCs (92%), and overexpression of EGFR in FL-HCC cells was considered to occur by gene amplification rather than by polysomy.[17] Therefore, a new strategy using a monoclonal antibody against EGFR should be advanced

TABLE 2. FL-HCC Presenting With Gynecomastia in Pediatric Patients in English Literature

Author	Age (y)	History of Breast Enlargement	Tumor Size (cm), Location	Operation	Chemotherapy	Estradiol (pg/mL)	Outcome
Smith et al[13]	13.8	Unknown	9.5×11.2, right lobe	Resected (trisegmentectomy)	+	8.1	Alive (10 mo)
Agarwal et al[9]	17.5	5.5	φ15, right lobe φ3.6, quadrate lobe Metastasis to left lung	Completely resected	+	312	Recurrent (1 y)
Sher et al[14]	13.8	1.5	Unknown	Unknown	Unknown	105.96	Unknown
Hany et al[10]	15	3	Multiple metastases abdominal and lung	Nonresectable	CDDP doxyorubicin taxol	16.6	Died
McCloskey et al[11]	13.8	1.5	13×12.5×8.5, right lobe	Resected	CDDP adriamycin 5-FU	106	Alive (5 mo)

FL-HCC indicates fibrolamellar hepatocellular carcinoma.

as a candidate for effective therapy against such cancers as colorectal carcinoma.[18] Although there is currently no effective therapy against FL-HCC other than surgical resection,[1,2,5] cetuximab may be more beneficial because there was no activating mutation in EGFR.[19] In addition, sorafenib which inhibits tumor neoangiogenesis via the raf-mek-erk signaling pathway and vascular endothelial growth factor and platelet-derived growth factor receptors signaling pathways, was recently reported to delay disease progression in advanced HCC.[12] Furthermore, expression of both EGFR and aromatase in FL-HCC cells is very intriguing and has been reported at the mRNA level. But the authors are the first to show it at the protein expression level.

An earlier study of liver cancer cell growth in vitro suggested that growth was promoted by aromatase-induced estrogen via both estrogen receptor α and EGFR.[20] In fact, overexpression of both EGFR and estrogen receptor α were independent, poor prognostic factors in nonsmall cell lung cancer.[21] Based on these reports, cases that present with both gynecomastia and EGFR overexpression, as in our patient, may be concerning for poor prognosis.

REFERENCES

1. Torbenson M. Review of the clinicopathologic features of fibrolamellar carcinoma. *Adv Anat Pathol.* 2007;14:217–223.
2. Stipa F, Yoon SS, Liau KH, et al. Outcome of patients with fibrolamellar hepatocellular carcinoma. *Cancer.* 2006;106:1331–1338.
3. Hernandez-Castillo E, Mondragon-Sanchez R, Garduno-Lopez AL, et al. Hepatocellular carcinoma in the youth. A comparative analysis with hepatocellular carcinoma in adulthood. *Hepatogastroenterology.* 2005;52:903–907.
4. Katzenstein HM, Krailo MD, Malogolowkin MH, et al. Fibrolamellar hepatocellular carcinoma in children and adolescents. *Cancer.* 2003;97:2006–2012.
5. Pinna AD, Iwatsuki S, Lee RG, et al. Treatment of fibrolamellar hepatoma with subtotal hepatectomy or transplantation. *Hepatology.* 1997;26:877–883.
6. Kakar S, Burgart LJ, Batts KP, et al. Clinicopathologic features and survival in fibrolamellar carcinoma: comparison with conventional hepatocellular carcinoma with and without cirrhosis. *Mod Pathol.* 2005;18:1417–1423.
7. Colquhoun AJ, Mellon JK. Epidermal growth factor receptor and bladder cancer. *Postgrad Med J.* 2002;78:584–589.
8. Buckley AF, Burgart LJ, Sahai V, et al. Epidermal growth factor receptor expression and gene copy number in conventional hepatocellular carcinoma. *Am J Clin Pathol.* 2008;129:245–251.
9. Agarwal VR, Takayama K, Van Wyk JJ, et al. Molecular basis of severe gynecomastia associated with aromatase expression in a fibrolamellar hepatocellular carcinoma. *J Clin Endocrinol Metab.* 1998;1797–1800.
10. Hany MA, Betts DR, Schmugge M, et al. A childhood fibrolamellar hepatocellular carcinoma with increased aromatase activity and a near triploid karyotype. *Med Pediatr Oncol.* 1997;28:136–138.
11. McCloskey JJ, Germain-Lee EL, Perman JA, et al. Gynecomastia as a presenting sign of fibrolamellar carcinoma of the liver. *Pediatrics.* 1988;82:379–382.
12. Iovet JM, Ricci S, Mazzaferro V, et al. Sorafenib in advanced hepatocellular carcinoma. *N Engl J Med.* 2008;359:378–390.
13. Smith MT, Blatt ER, Jedlicka P, et al. Best cases from the AFIP: fibrolamellar hepatocellular carcinoma. *Radiographics.* 2008;28:609–613.
14. Sher ES, Migeon CJ, Berkovitz GD. Evaluation of boys with marked breast development at puberty. *Clin Pediatr (Phila).* 1998;37:367–371.
15. Nicholson RI, Gee JM, Harper ME. EGFR and cancer prognosis. *Eur J Cancer.* 2001;37(suppl 4):S9–S15.
16. Spano JP, Lagorce C, Atlan D, et al. Impact of EGFR expression on colorectal cancer patient prognosis and survival. *Ann Oncol.* 2005;16:102–108.
17. Buckley AF, Burgart LJ, Kakar S. Epidermal growth factor receptor expression and gene copy number in fibrolamellar hepatocellular carcinoma. *Hum Pathol.* 2006;37:410–414.
18. Mitchell P. Erbitux diagnostic latest adjunct to cancer therapy. *Nat Biotechnol.* 2004;22:363–364.
19. Karapetis CS, Khambata-Ford S, Jonker DJ, et al. K-ras mutations and benefit from cetuximab in advanced colorectal cancer. *N Engl J Med.* 2008;359:1757–1765.
20. Carruba G. Aromatase in nontumoral and malignant human liver tissues and cells. *Ann N Y Acad Sci.* 2009;1155:187–193.
21. Kawai H, Ishii A, Washiya K, et al. Combined overexpression of EGFR and estrogen receptor alpha correlates with a poor outcome in lung cancer. *Anticancer Res.* 2005;25:4693–4698.

Evaluation of contrast-enhanced ultrasonography using perfluorobutane (Sonazoid®) in patients with small hepatocellular carcinoma: Comparison with dynamic computed tomography

MIKI KAN[1], ATSUSHI HIRAOKA[2], TAKAHIDE UEHARA[2], SATOSHI HIDAKA[2], MISA ICHIRYU[2], HIROMASA NAKAHARA[2], HIRONORI OCHI[2], ATSUSHI TANABE[2], AKIHIRO KODAMA[2], AKI HASEBE[2], YASUYUKI MIYAMOTO[2], TOMOYUKI NINOMIYA[2], MASANORI ABE[3], YOICHI HIASA[3], BUNZO MATSUURA[3], MORIKAZU ONJI[3], YUKI SHINBATA[1], CHIEKO KAMEOKA[1], SHIGEKAZU DOI[1], HIROMI TAMURA[1], KEIZOU FURUYA[1] and KOJIRO MICHITAKA[2]

Departments of [1]Medical Laboratory, and [2]Gastroenterology, Ehime Prefectural Central Hospital; [3]Department of Gastroenterology and Metabology, Ehime University Graduate School of Medicine, Ehime, Japan

Received November 30, 2009; Accepted February 8, 2010

DOI: 10.3892/ol_00000085

Abstract. This study aimed to elucidate the efficacy of contrast-enhanced ultrasonography (CEUS) with perfluorobutane (Sonazoid®) in the diagnosis of hepatocellular carcinomas (HCCs), particularly small HCCs, by comparing the results with dynamic computed tomography (Dy-CT). Seventy-nine nodules in 69 patients with chronic liver disease, suspected as HCCs were studied. The nodules were selected based on the results of B-mode ultrasonography and/or Dy-CT conducted between January and August 2007. The nodules were divided into two groups: the S-group with tumors ≤2 cm (49 nodules), and the L-group with tumors >2 cm (30 nodules). Typical HCCs were defined, and the nodules were enhanced and shown as defects in the arterial and late phase of Dy-CT, respectively. Target lesions were scanned using CEUS, and the results were compared with those of Dy-CT. The L-group nodules diagnosed as HCCs using Dy-CT were also diagnosed as HCCs using CEUS. In the S-group, the diagnostic sensitivity of CEUS was 94.7% and the specificity was 81.8%. We diagnosed two liver tumors that were detected by CEUS but not by Dy-CT; biopsies revealed one tumor to be a well-differentiated HCC and the other to be an atypical adenomatous hyperplasia. The sensitivity and specificity of CEUS against HCC were high even in the small-size HCCs. Thus, Sonazoid is useful in the screening for small HCCs.

Correspondence to: Dr Kojiro Michitaka, Department of Gastroenterology, Ehime Prefectural Central Hospital, Kasuga-Cho 83, Matsuyama City, Ehime 790-0024, Japan
E-mail: kojiromichitaka@gmail.com

Key words: Sonazoid®, perfluorobutane, hepatocellular carcinoma, contrast-enhanced ultrasonography, dynamic computed tomography

Introduction

Dynamic computed tomography (Dy-CT) and conventional B-mode ultrasonography (US) are used for the screening of hepatocellular carcinomas (HCCs). Although Dy-CT is useful for assessing the vascularity of hepatic tumors, negative aspects include exposure to X-rays and the high cost. On the other hand, B-mode US is economical and easy to perform repeatedly. However, some nodules are difficult to identify or diagnose, particularly small-size tumors, due to the sensitivity as well as the irregularity in the case of chronic injured liver.

Recently, the development of US and contrast-enhanced ultrasonographic agents for hepatic tumors have enabled the diagnosis of HCC in the early stage. Perfluorobutane (Sonazoid®) (1) was approved as a new contrast-enhanced ultrasonographic agent in Japan in January 2007. The tumors are phagocyted by Kupffer cells after injection. The primary characteristic of this agent is the ability to maintain observations continuously as the tumors are being phagocyted by Kupffer cells. The present study evaluated the diagnostic efficacy of contrast-enhanced (CE) US with Sonazoid for HCCs, particularly small-size HCCs.

Materials and methods

Seventy-nine nodules detected by US and/or Dy-CT between January and August 2007 in 70 patients examined at Ehime Prefectural Central Hospital, Japan, were studied. Nodules showing the typical findings of liver hemangioma were excluded from this study. Informed consent was obtained from all of the studied patients and the study protocol was approved by the Ethics Committee of Ehime Prefectural Central Hospital.

CEUS was performed within 1 month from the Dy-CT examination in all of the patients. We divided the nodules into two groups. Forty-nine nodules (41 patients) ≤2 cm in diameter were defined as the S-group, and 30 nodules (28 patients) >2 cm in diameter were defined as the L-group. Sonazoid was

Table I. Technical background using the extended pure harmonic detection method and ProSound Alpha-10.

Image	Frequency (MHz)	MI index	Range	Gain	Contrast
Fundamental	5.00	0.30	17	60	15
Contrast	1.88	0.24	17	45	18

MI, mechanical index.

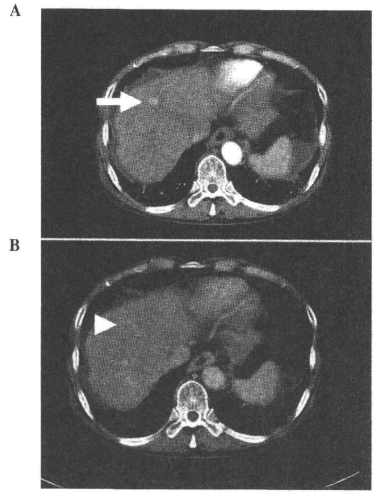

Figure 1. A nodule diagnosed as a typical hepatocellular carcinoma by dynamic computed tomography. (A) The nodule was enhanced in the arterial phase (arrow) and (B) revealed as a defect in the late phase (arrowhead).

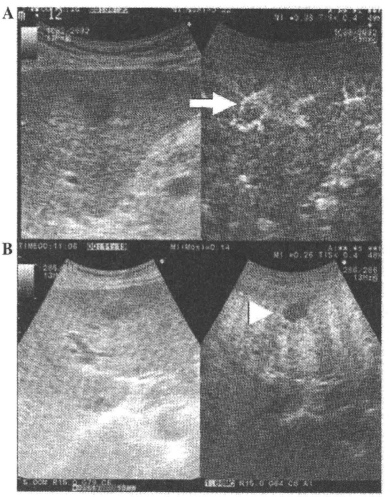

Figure 2. A nodule diagnosed as a typical hepatocellular carcinoma by contrast-enhanced ultrasonography. (A) The nodule was enhanced in the arterial phase (arrow) and (B) revealed as a defect in the Kupffer phase (arrowhead).

used as the contrast-enhanced ultrasonographic agent (4 μl/kg of body weight) in all examinations, and the target lesions were scanned after injection in the arterial and Kupffer phases using a ProSound Alpha-10 (Aloka Co. Ltd., Tokyo, Japan). The arterial phase of CEUS imaging was identified 10-60 sec after Sonazoid injection, and the Kupffer phase 10 min after the injection (2). ProSound Alpha-10 was set up in the extended pure harmonic detection mode and was used with a convex type probe (Table I). The results were compared retrospectively between CEUS and Dy-CT. Nodules were diagnosed as typical HCCs by Dy-CT when they were enhanced in the arterial phase and were revealed as a defect in the portal phase of Dy-CT (Fig. 1) (3). Moreover, a nodule was diagnosed as typical HCC, when it was shown as hypervascular in the arterial phase and revealed as a defect lesion in the Kupffer phase (Fig. 2) by CEUS (4,5).

Statistical analysis. Statistical analyses were carried out using the Chi-square test with StatView version 5.0 (SAS Institute, Inc., Berkeley, CA, USA). $P<0.05$ was considered statistically significant.

Results

The average diameter of the S-group nodules was 1.42±0.39 cm (range 0.8-2 cm), while that of the L-group was 3.03±1.10 cm (range 2.1-8 cm). The background of each patient is described in Table II. When typical HCCs using Dy-CT were defined as the gold standard of diagnosing HCCs, the sensitivity and specificity of CEUS with Sonazoid were 97.1% (66/68) and 81.8% (9/11), respectively (Table III). The sensitivity and specificity in the S-group were 94.7% (36/38) and 81.8% (9/11), respectively, while the positive and negative predictive values were 94.7% (36/38) and 81.8% (9/11), respectively. In the L-group, the nodules were diagnosed as HCCs by CEUS, which was identical with the results of Dy-CT.

In the S-group, 2 nodules were detected by CEUS, but were not detected by Dy-CT. On the other hand, 2 nodules

Table II. Background of the patients.

	S-group[a]	L-group[b]
Male	25	20
Female	16	8
Mean age (years)	71.1±7.4	71.0±9.0
Positive for anti-HCV	38	21
Positive for HBsAg	0	5
Positive for both anti-HCVAb and HBsAg	3	0
Negative for both anti-HCVAb and HBsAg	0	2
Past history of HCC		
Positive	16	11
Negative	25	17
No. of tumors	49	30
Tumor size (cm)	1.42±0.39	3.03±1.10
AST (IU/l)	73.6±100.9	66.8±42.5
ALT (IU/l)	52.3±55.9	51.4±31.3
T-bil (mg/dl)	0.92±0.47	1.07±0.80
TP (g/dl)	7.3±0.8	7.1±0.7
ALB (g/dl)	3.7±0.6	3.7±0.6
PLT ($*10^4/\mu l$)	11.8±6.10	13.3±8.9
PT (%)	72.1±10.4	74.5±14.4
AFP	89.4±300.0	142.1±360.8

[a]HCC diameter ≤2 cm. [b]HCC diameter >2 cm. anti-HCV Ab, anti-hepatitis C virus antibody; HBsAg, hepatitis B virus surface antigen; HCC, hepatocellular carcinoma; AST, aspartate aminotransferase; ALT, alanine aminotransferase; T-bil, total bilirubin; TP, total protein; ALB, albumin; PLT, platelets; PT, prothrombin time and AFP, α fetoprotein.

Table III. Comparison between contrast enhanced ultrasonography and dynamic computed tomography.
A, All cases.

	Dy-CT		
	Typical HCC	Not typical HCC	Total
CEUS			
Typical HCC	66	2[a]	68
Not typical HCC	2[b]	9	11
Total	68	11	79

B, S-group.

	Dy-CT		
	Typical HCC	Not typical HCC	Total
CEUS			
Typical HCC	36	2[a]	38
Not typical HCC	2[b]	9	11
Total	38	11	49

C, L-group.

	Dy-CT		
	Typical HCC	Not typical HCC	Total
CEUS			
Typical HCC	30	0	30
Not typical HCC	0	0	0
Total	30	0	30

[a]One case was diagnosed as a well-differentiated hepatocellular carcinoma, and the other was diagnosed as an atypical adenomatous hyperplasia by biopsy. [b]The nodule was located in a deep position. HCC, hepatocellular carcinoma; CEUS, contrast-enhanced ultrasonography and Dy-CT, dynamic computed tomography.

were detected by Dy-CT, but not by CEUS. We performed US-guided biopsies in the 2 nodules which were undetected by Dy-CT. One was detected as a mixed echoic nodule with a diameter of 0.8 cm in segment 5 of the liver by B-mode US (male, 63 years of age, positive for anti-HCVAb). This nodule was revealed as a hypervascular lesion in the arterial phase and as a defect in the Kupffer phase. Based on the CEUS findings, the tumor was suspected to be HCC (typical HCC by CEUS). The result of the biopsy identified it as a well-differentiated HCC. The other nodule was revealed to be hypoechoic with a diameter of 1 cm in segment 8 of the liver by B-mode US (female, 81 years of age, positive for anti-HCVAb). The tumor was slightly enhanced peripherally in the arterial phase and was revealed as a partial defect in the Kupffer phase by CEUS. The CEUS findings were not conclusive, and this tumor was unable to be diagnosed as a typical HCC. The result of the biopsy identified it as an atypical adenomatous hyperplasia (AAH). Among the 38 nodules detected by CEUS, the diameter of 8 nodules including the above-mentioned 2 nodules were <1 cm. The other 6 nodules larger by <1 cm were diagnosed as typical HCCs by both Dy-CT and CEUS. One nodule detected by Dy-CT but not by CEUS was located in a deep position from the body surface.

Discussion

Sonazoid is a new agent for CEUS which reveals the arterial flow in tumors. Moreover, malignant hepatic tumors can be observed continuously and repeatedly throughout the examination as a defective area in the Kupffer phase due to the lack of Kupffer cells in tumors (6).

Classic HCC cases have a blood flow from the feeding artery and a decrease in or lack of a portal vein in the tumor, whereas those in the early stage have a portal vein and increased arterial flow. When the diameter of the tumor expands, the portal flow and Kupffer cells decrease in the tumor (7,8). The present study validated the usefulness of

CEUS using Sonazoid. We diagnosed all nodules as typical HCCs in cases with tumors >2 cm in diameter (L-group) using CEUS, identical to the results obtained using Dy-CT. Therefore, it was confirmed that the diagnostic ability for detecting HCCs with a diameter >2 cm using CEUS with Sonazoid was identical to Dy-CT.

A small HCC can be difficult to diagnose. We performed CEUS with Sonazoid to evaluate small HCC nodules ≤2 cm in diameter (S-group) and found the sensitivity and specificity to be 94.7 and 81.8%, respectively, while the positive and negative predictive values were 94.7 and 81.8%, respectively. Although the study population was small and the study design was retrospective, the results were encouraging.

The high rates for sensitivity and specificity of CEUS with Sonazoid are thought to depend on the continuous view provided in the Kupffer phase. CEUS with other agents (e.g., Levovist® and SonoVue®) does not reveal the Kupffer phase image continuously for >10 min, as the imaging of the Kupffer phase is performed by bursting microbubbles that accumulate in Kupffer cells by sound waves (9). Continuous viewing in the Kupffer phase image with Sonazoid can be obtained since the images are obtained with vibration, rather than bursting by sound waves, which makes it easy to observe abnormal findings (10).

Wang *et al* (9) reported on CEUS imaging with Levovist. A combination of the characteristics of arterial phase enhancement and the absence of the Kupffer phase enhancement as determined by CEUS was highly specific for small HCCs in cirrhosis patients. However, the use of CEUS with Levovist is difficult for many operators since the enhancement of the Kupffer phase vanishes immediately, and the scan cannot be conducted continuously. Sonazoid is considered to be superior for the evaluation of hepatic tumors compared with other agents, since nodules that are invisible in B-mode but visible in Dy-CT are not detected in the Kupffer phase with a continuous view due to the character of Sonazoid. the detection of the target lesion, we observed the arterial flow by re-injection into the defect area (11). Hohmann *et al* reported that SonoVue markedly improved the characterization of focal hepatic lesions in comparison with unenhanced sonography (12). Giorgio *et al* reported that the enhancement pattern related to tumor hypervascularity as well as sensitivity and specificity with SonoVue were high for nodules 1-3 cm in diameter, whereas these were very low (sensitivity, 27.3%; specificity, 100%) for nodules <1 cm (13).

In the present study, 8 nodules were <1 cm and detectable by CEUS with Sonazoid. Two nodules, which were invisible by Dy-CT but visible in the Kupffer phase of CEUS, were diagnosed as a well-differentiated HCC and an AAH. This indicates that certain HCC nodules which are not detectable by Dy-CT may be detectable by CEUS. The characteristics of these nodules should be investigated. Although these 2 nodules were diagnosed by biopsy, another 6, which were <1 cm, were diagnosed as typical HCCs by CEUS with Sonazoid.

There are several negative aspects associated with CEUS, such as the difficulty in discerning lesions deeply positioned, liver surface lesions confirmed by US, and lesions located in the blind spot. In addition, the internal echo is very irregular in the case of chronic liver injury. While all nodules of the L-group were detected by CEUS, 2 nodules in the S-group were not as they were located in a deep position. The diagnostic efficacy for small HCCs is evident when understanding the characteristics and disadvantages of CEUS particularly in the Kupffer phase.

In conclusion, the low cost and non-invasive characteristics of CEUS with Sonazoid are useful in screening examinations and for diagnosing small HCCs.

References

1. Sontum PC: Physiochemical characteristics of Sonazoid, a new contrast agent for ultrasound imaging. Ultrasound Med Biol 34: 824-833, 2008.
2. Watanabe R, Matsumura M, Chen CJ, *et al*: Characterization of tumor imaging with microbubble-based ultrasound contrast agent, Sonazoid, in rabbit liver. Biol Pharm Bull 28: 972-977, 2005.
3. Bruix J and Sherman M: Management of hepatocellular carcinoma. Hepatology 42: 1208-1236, 2005.
4. Watanabe R, Matsumura M, Munrmasa T, *et al*: Mechanism of hepatic parenchyma-specific contrast of microbubble-based contrast agent for ultrasonography: microscopic studies in rat liver. Invest Radiol 42: 643-651, 2007.
5. Kindberg GM, Tolleshaug H, Roos N, *et al*: Hepatic clearance of Sonazoid perfluorobutane microbubbles by Kupffer cells does not reduce the ability of liver to phagocytose or degrade albumin microspheres. Cell Tissue Res 312: 49-54, 2003.
6. Kudo M: New sonographic techniques for the diagnosis and treatment of hepatocellular carcinoma. Hepatol Res 37 (Suppl 2): 193-199, 2007.
7. Nakashima O, Sugihara S, Kage M, *et al*: Pathomorphologic characteristics of small hepatocellular carcinoma: a special reference to small hepatocellular carcinoma with indistinct margins. Hepatology 22: 101-105, 1995.
8. Matsui O, Kadoya M, Kameyama T, *et al*: Benign and malignant nodules in cirrhotic livers: distinction based on blood supply. Radiology 178: 493-497, 1991.
9. Wang JH, Lu SN, Hung CH, *et al*: Small hepatic nodules (< or =2 cm) in cirrhosis patients: characterization with contrast-enhanced ultrasonography. Liver Int 26: 928-934, 2006.
10. Numata K, Morimoto M, Ogura M, *et al*: Ablation therapy guided by contrast-enhanced sonography with Sonazoid for hepatocellular carcinoma lesions not detected by conventional sonography. Ultrasound Med 27: 395-406, 2008.
11. Minami Y, Chung H, Kudo M, *et al*: Radiofrequency ablation of hepatocellular carcinoma: value of virtual CT sonography with magnetic navigation. Am J Roentgenol 190: W335-W341, 2008.
12. Hohmann J, Skrok J, Puls R, *et al*: Characterization of focal liver lesions with contrast-enhanced low MI real time ultrasound and SonoVue. Rofo 175: 835-843, 2003.
13. Giorgio A, De Stefano G, Coppola C, *et al*: Contrast-enhanced sonography in the characterization of small hepatocellular carcinomas in cirrhotic patients: comparison with contrast-enhanced ultrafast magnetic resonance imaging. Anticancer Res 27: 4263-4269, 2007.

Biomedical Research 2010; 21 (3): 230-232

Case report: Immunohistochemical characterization of pulmonary corpora amylacea in an autopsy case, with special reference to its pathogenesis

Yuji Ohtsuki[1], Toshiharu Maeda [2], Yoshiko Soga[2], Keizo Furuya[2], Yuhei Okada[1], Gang-Hong Lee[3], Mutsuo Furihata[3]

[1]Division of Pathology, Matsuyama-shimin Hospital, Matsuyama, Ehime, Japan
[2]Department of Diagnostic Pathology, Ehime Prefectural Central Hospital, Matsuyama, Ehime, Japan
[3]Department of Pathology, Kochi Medical School, Kochi University, Kochi, Japan

Abstract

Pulmonary corpora amylacea (PCA) is rare. We report here an autopsy case of a Japanese woman in her eighties who harbored numerous PCAs in both lungs. Multiple infarctions were found in the brainstem as the cause of her death. In an attempt to characterize these PCAs, several antibodies were used, including those to surfactant protein (SP)-A, SP-D, KL-6, epithelial membrane antigen (EMA), pancytokeratins, and macrophages. PCAs were almost all positive for SP-A, in concentric lamellar fashion, some with niduses. Internal positivity of PCAs was observed on diastase-digested PAS reaction. Staining for SP-D was negative. More than half of the PCAs were covered by macrophages, indicating that they were foreign bodies. With regard to the pathogenesis of PCAs, we believe that SP-A is one of the important factors whether niduses are present or absent, and that SP-A is gradually deposited on the surfaces of PCAs in lamellar fashion.

Our findings indicate that SP-A is required for the formation of PCAs, and suggest that pulmonary dysfunction, leading to an imbalance between the production of SP-A and its absorption, might be the cause of the deposition of PAS-positive glycoproteins and/or SP-A as PCAs.

Key words: Lung, corpora amylacea, immunohistochemistry, pathogenesis

Accepted January 01 2001

Introduction

Pulmonary corpora amylacea (PCA) is a rare condition, and is detected especially in the elderly, at a frequency of 0.6%–3.8% of autopsies [1,2]. Some studies have reported that the pathogenesis of PCAs involves the degeneration of pulmonary macrophages[3] or needs the formation of niduses 2,4]. PCAs have been proven to express the surfactant protein-A (SP-A) [5] and epithelial membrane antigens (EMA) [6]. In this study, we analyzed PCAs by performing detailed immunohistochemical studies using several antibodies, including antibodies against SP-A, surfactant protein D (SP-D), EMA and KL-6. Then, the comparison of both PCAs and prostatic amyloid bodies were also performed on the stainability with SP-A antibody. We propose a hypothesis for the pathogenesis of PCAs on the basis of the results of immunohistochemical studies, especially those using SP-A.

Case Report

We report the case of an 81-year-old female with cerebral infarction. On autopsy, we detected infarcted foci in left thalamus , cereberum and medulla oblongata as the cause of death(whole brain 1120g). Then, many PCAs were found in both lung (265g, lt., 325g, rt.), combining focal diffuse alveolar damage pattern with superimposed bronchopneumonia. PCAs were detected incidentally during histopathological examination of pulmonary tissues. Besides routine Hematoxylin-Eosin stain(H&E), periodic acid Schiff reaction with diastase digestion and congo red stain were performed. Then, amyloid bodies in prostatic tissues of nodular hyperplasia from three patients, each seventieth or eightieth in ages, were also used in order to compare those with SP-A stainability.

Immunohistochemical staining was performed using the

labeled streptavidin-biotin complex (LSABC) method, as described previously[7,8]. We used antibodies to SP-A (clone PE10, 1:50, no pretreatment (NP); Dako, Kyoto, Japan), SP-D[9] (1:1600, autoclaved (AC); kindly provided by Yamasa, Chousi, Japan), KL-6 (1:5120, NP; kindly provided by Eisai Co., Tokyo, Japan), EMA (Dako-EMA, E29, 1:50, microwave pretreatment; Dako, Kyoto, Japan,), pancytokeratin AE1/AE3 (1:400, pretreated with pronase (P); Boehringer-Mannheim Biochemical, Germany), and macrophage-associated antigen CD68 (1:50, P

Pathology

Routine HE staining of lung tissues revealed PCAs of eosinophilic round or ellipsoid bodies (diameter, 50–100 um). These bodies were detected in the airspace, including respiratory bronchioles and alveolar ducts (Fig. A). The isolated PCAs were positive for the periodic acid-Schiff (PAS) reaction, and some of them contained black granular niduses (Fig. B). Staining with Congo red revealed pinkish needle-shaped nidus-like structures having birefringence at the center of the PCAs (Fig. C, arrow). The central nidus-like structures were present in almost one-third of the detected PCAs in total (45 out of 167, 26.9%). AE1/AE3 immunostaining revealed that only a few PCAs (8 out of 181, 6.1%) were surrounded by more than 2 epithelial cells (Fig. D). However, CD68 immunostaining revealed

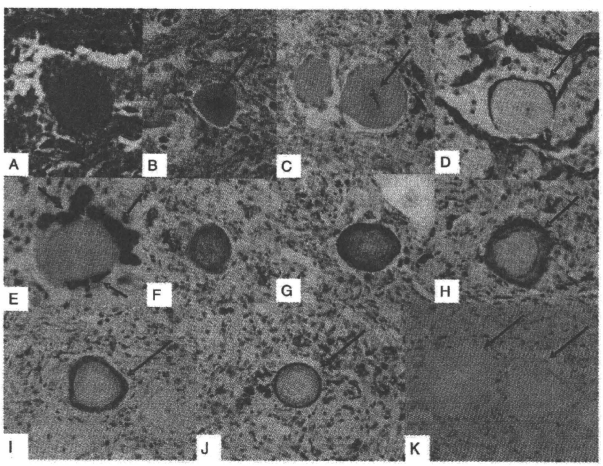

Figure 1. *Light-microscopy findings of pulmonary corpora amylacea (PCA). Note: eosinophilic round bodies with concentric layers in a respiratory bronchiole (A). PCA containing black granular nidus□B, arrow) was positive for the periodic acid-Schiff (PAS) reaction. On staining with Congo red, the nidus was stained positively (C, arrow) with birefringence. A few PCA were surrounded by epithelial cells (D, arrow); these were positive for pancytokeratin AE1/AE3 antibody. CD68-positive macrophages covered almost half the number of PCA (E, arrow). PCA positive for the SP-A antibody had various features (F,-J): outer positive concentric layers with central negativity (H, I, J, arrows). PCA were negative for SP-D immunostaining (K, arrows). A: H&E staining; B: PAS reaction; C: Congo red staining; D–K: Labeled streptavidin-biotin complex (LSABC) method; A–D, F–K: ×200; E: ×400 in original magnification*

that more than 2 macrophages were associated with almost half the number of PCAs (74 out of 163, 45.4%) (Fig. E). SP-A staining revealed several remarkable findings; PCAs were stained in various patterns such as partial or total concentric rings and doughnut-shaped patterns with central-negativity (Fig. F-J). Of the 155 detected PCAs, only 2 (1.3%) PCAs were completely negative for SP-A staining. As controls, prostatic tissue samples from 3 cases of prostatic nodular hyperplastic lesions with amyloid bodies in the glandular spaces were stained for SP-A; these samples were completely negative for SP-A. This observation suggested that prostatic amyloid bodies were different from PCA. SP-D was not detected in the PCA (Fig. K). Although the internal EMA-negativity of PCAs in the present study can not be explained at present, the findings of our study indicate that SP-A is very impor-

tant for the morphogenesis of PCAs, as evidenced.

Discussion

Histopathologically, some PCAs contained needle-shaped niduses (Fig. F and J), and the cores of the PCAs were found to be composed of niduses and PAS-positive glycoproteins. Then, SP-A deposition was demonstrated on the surfaces of PCAs in thin or thick concentric layers. Therefore, the surfaces of PCA were composed of SP-A, while PAS-positive glycoproteins comprised the interior; With regard to the pathogenesis of PCA, we believe that SP-A is an important factor irrespective of the presence or absence of nidus and that SP-A is gradually deposited on the surfaces of PCAs in a lamellar fashion. Previous studies have reported that the regenerating pulmonary epithelial type II cells[7] and coarse granules of pulmonary alveolar proteinosis (PAP) [10] were positive for staining with SP-D antibody. PCAs were stained superficially in a linear fashion with KL-6 and EMA antigens. A previous case study reported that, PCAs were positive for SP-A and EMA[6].However, concentric depositions of EMA and KL-6, which are fundamental components of the surface of airways[8], appeared to be deposited only on the surfaces of PCAs in a linear fashion. The contents of lymph vessels in PAP were stained positively for KL-6 and SP-D, indicating lymphatic drainage of KL-6 and SP-D [10].However, unlike the case of the study on PAP[10]., no significant findings in lymphatic vessels were detected in this study. The deposition of SP-A on the surfaces of PCAs and its absence in the lymph vessels in this study can be attributed to improper lymphatic drainage dué to pulmonary dysfunction. A few PCA were surrounded by epithelial cells, suggesting that epithelial cells do not likely grow on PCAs. Because almost half the number of PCAs were covered by macrophages, we concluded that they are recognized essentially as foreign bodies.

It is interesting to note that SP-A was almost exclusively positive for PCAs, but negative for SP-D; the reasons for this variable distribution are unknown. SP-A seems to exhibit some affinity for nidus-containing glycoproteins that are positive-for the PAS reaction. The presence of niduses and glycoproteins in the PCA cores and the deposition of SP-A on the surfaces of the PCA in a concentric fashion are vital observations of our study. Pulmonary dysfunction leading to an imbalance between the production of SP-A and its absorption mechanism might be the cause of the deposition of glycoproteins or SP-A as PCAs.

Acknowledgement

The authors would like to thank Mr. T. Watanabe, Ms. M. Izumimoto, and Ms. Y. Teratani for their excellent technical assistance. The authors would also like to express their gratitude to Ms. K. Takasuka and Ms. K. Yamamoto of the Matsuyama-shimin Hospital, Matsuyama, Japan for their secretarial assistance.

References

1. Michaelis L, Levine C.Pulmonary corpora amylacea. J Pathol Bacteriol 1957; 74: 49-56.
2. Hollander H, Hutchins GM. Central spherules in pulmonary corpora amylacea. Arch Pathol Lab Med 1978; 102: 629-630.
3. Dobashi M, Yuda F, Narabayashi M, et al. Histopathological study of corpora amylacea pulmonum. Histol Histopathol 1989; 4: 153-165.
4. Rocken C, Linke RP, Saeger W. Corpora amylacea in the lung, prostate and uterus. A comparative and immunohistochemical study. Pathol Res Pract 1996; 192: 998-1006.
5. Akino T, Mizumoto M, Shimizu H. et al. Pulmonary corpora amylacea contain surfactant apoprotein. Pathol Res Pract 1990; 186: 687-691.
6. Yamanouchi H, Yoshinouchi T, Watanabe R, et al. Immunohistochemical study of a patient with diffuse pulmonary corpora amylacea detected by open lung biopsy. Intern Med 1999; 38: 900-903.
7. Ohtsuki Y, Nakanishi N, Fujita J, et al. Immunohistochemical distribution of SP-D, compared with those of SP-A and KL-6, in interstitial pneumonias. Med Mol Morphol 2007; 40: 163-167.
8. Ohtsuki Y, Fujita J, Hachisuka Y, et al. Immunohistochemical and immunoelectron microscopic studies of the localization of KL-6 and epithelial membrane antigen(EMA) in presumably normal pulmonary tissue and in interstitial pneumonia. Med Mol Morphol 2007; 40: 198-202.
9. Inoue T, Matsuura E, Nagata A, et al. Enzyme-linked immunosorbent assay for human pulmonary surfactant protein D. J Immunol Methods 1994;173: 157-164.
10. Ohtsuki Y, Kobayashi M, Yoshida S, et al. Immunohistochemical localization of surfactant proteins A and D, and KL-6 in pulmonary alveolar proteinosis. Pathology 2008;40: 536-539.

Correspondence to:

Yuji Ohtsuki
Division of Pathology
Matsuyama-shimin Hospital
Matsuyama, Ehime 790-0067
Japan
Phone: +81-89-943-1151 Fax: +81-89-947-0026
E-mail: y.ohtsuki@matsuyama-shimin-hsp.or.jp

厚生労働科学研究費補助金（がん臨床研究事業）
分担研究報告書

バーチャルスライドシステムを用いた病理学教育に関する研究

研究分担者　森谷 卓也　　川崎医科大学医部医学科　教授

研究要旨

臨床医学で取り上げられる様々な疾患の病態を理解するためには、基礎医学教育の段階で、各臓器についてマクロからミクロのレベルまで系統的な形態学的観察を行うことが望ましい。川崎医科大学の現代医学教育博物館では、医学生・医療系学生向けの各種教材を製作しているが、これまではマクロ臓器に主眼を置いており、ミクロレベルの展示物との間に乖離を生じていた。この度、博物館内にバーチャルスライドシステムを導入したので、その利用法について検討した。第一に、医学部および学園内の関連学科における顕微鏡実習用のライブラリを構築することで、学生が任意にアクセスし自己学習を行ったり、専用のコンピューター実習室を利用して試験を実施することが可能となった。第二に、バーチャルスライドから取り込んだ顕微鏡画像を大判用紙に出力し、展示物として利用することが可能となった。スペースが確保できれば、段階を追って異なる倍率を示す必要がなくなり、マクロ臓器（またはマクロ画像）のみならず放射線画像等とも同時に、精細画像を供覧できるものと思われた。第三に、病理肉眼標本等にバーコードを貼付けて、バーコードリーダーを接続したパソコンでスキャンすることによって、顕微鏡画像の詳細なデータや解説を直ちに見て学ぶことができると考えられた。

A.研究目的

臨床医学で取り上げられる様々な疾患の病態を理解するためには、疾患の形態学的異常と、機能的障害の要素を適宜組み合わせて学ぶ必要がある。このうち、形態学的な病態の把握は、マクロ像からミクロ像までを連動させて理解することが望ましいが、マクロ所見はそのまま観察可能であるのに対して、ミクロ画像は染色の実施と顕微鏡操作が加わるために、学生にとっては必ずしも理解が容易ではないのが実情と思われる。マクロ像については、昨今の画像診断のめざましい発展の結果、その十分な理解は極めて重要な因子になってきてはいるが、実物の臓器を観察する機会は案外乏しいと思われる。ミクロに至ってはさらに、マクロとは別次元の観察物のように理解されてしまい、弱拡大（マクロや画像診断との対比）よりも強拡大の細胞所見がより重要視される傾向も危惧される。また、いわゆる「顕微鏡嫌い」の学生にとっては、ミクロ観察自体が苦痛というよりも、顕微鏡操作そのものに慣れないために苦手意識が生じている者も少なくないと考えられる。このような、形態学教育における問題点を解決ないし改善するために、バーチャルスライド導入の意義を検討し、とりわけ、われわれの施設に特異的な、博物館での利用法について考察した。

B.研究方法

バーチャルスライドシステムは、オリンパス社のVS-100を用いた。顕微鏡画像は対物40倍でスキャンし、画像を取り込んだ。

検討１：病理組織実習（顕微鏡実習）での利用：医科大学2学年および3学年の病理組織実習用に顕微鏡画像を取り込み、学内サーバーにデータを保存した。顕微鏡実習および実習試験は、学生個人がそれぞれ備え付けのパソコンを利用可能な、マルチメディア教室を利用して行った。パソコンには予め専用の閲覧ソフト（OlyVIA）をインストールし、学生には専用のパスワードを付与してアクセスできるようにした。

検討２：スキャン画像のパネル展示：スキャン

したタイリング画像全体を、大判画像（A1サイズ）として出力した。また、同一症例の肉眼画像、顕微鏡強拡大像なども同様に出力し、組み合わせてパネル展示した。

検討３：マクロ臓器と連動させたライブラリとしての利用：病理肉眼標本にバーコードを貼り付けて、パソコンに接続したバーコードリーダーでスキャンした。スキャンの結果、パソコンソフトが起動して、当該症例のバーチャルスライドデータに直接アクセスできるようにセットした。

（倫理面への配慮）

博物館の展示物は生検・手術材料の場合は患者から、病理解剖の場合は遺族から、研究および教育目的での二次利用に関し、書面による同意を得た。使用に際しては個人情報に配慮し、連結可能不特定化を行った。

C.研究結果

検討１：バーチャルスライドは全員が一度に観察可能であること、全く同一の標本を観察できること、その結果解説も全員に均一な情報を提供できること、退色や破損の心配がないこと、など利点が多くみられた。学生にとっては、パソコンの操作に躊躇が見られたのは初回実習のみで、以後は操作手順書を用いて各人が自由にアクセス可能となった。数回の実習終了後に挙手によって調査したところ、顕微鏡を用いた実習に戻りたいと主張した学生はほぼ皆無であった。

検討２：バーチャルスライドの、タイリング画像（スキャン画像）をA1版に大判出力し、それらをマクロ画像、ルーペ像、強拡大画像と組み合わせて展示した。マクロ画像と、同一面のミクロ画像の対比は有用であった。ルーペ像と、バーチャルスライドのタイリング画像は、全く同じ素材で引き伸ばし率が異なっている状態だったが、タイリング画像は大判に引き伸ばしてもフォーカスがずれることはなかった。右下に強拡大像の写真を追加展示してはあるが、タイリング画像の場合、写真に近づいたりやや離れて観察することによって、顕微鏡の倍率を変えて観察するのと相同の効果が得られ、一枚の画像で弱拡大（ルーペ像）から強拡大（個々の細胞所見）までを、自由に観察することが可能であった。

検討３：バーコードリーダー付きのパソコンを用意し、マクロ臓器の標本ケースに貼り付けたバーコードを読み取ると、症例の解説画面が現れるようにセットした。さらに、希望により顕微鏡画像をクリックすれば、無線LANを通じてサーバーに接続し、バーチャルスライドが閲覧できるようにした。実際の臓器を同時に観察でき、バーチャルスライドの操作によって自由に倍率や視野を変えて、マクロ像などと比較しながら観察することができた。

D.考察

顕微鏡実習におけるバーチャルスライドの応用は、最近様々な大学で導入されており、概ね良好な結果が得られている。現代の学生はパソコン操作にも十分慣れており、使用すること自体については、ほとんど問題は見当らなかった。現在われわれが用いている仕様では、デジタルデータは全て学内の専用サーバー上にあり、専用ソフトを用いて、定められた場所でのみ閲覧が可能となっている。セキュリティー上の問題を解決する必要はあるが、可能であれば、パスワードを使って学外からの閲覧が可能となれば、学生が自習するうえでも有用である。現在は、自習用として実習内容を解説したCD-ROMを配布しているが、将来的には全てオンラインで閲覧し、勉強できるようになれば良いと考える。

検討２および３は、博物館展示に関連する内容であり、われわれの施設に特異的な事象である。一般に、展示物の閲覧は、閲覧者（来館者）自身による操作のステップが極力少なく、単純であるほうが良いと思われる。常識的には、ミクロ画像は専用機器である顕微鏡を必要とし、それを観察するためには若干の技術を必要とする。しかし、検討２におけるタイリング画像の大判プリントは、顕微鏡がなくても弱拡大から強拡大までを1枚の写真で観察可能であった。閲覧者自身が移動して観察しなければならないという若干の不都合はあ

るものの、展示を行う側からは大変提示がしやすい状況を作っていた。顕微鏡画像を大きく引き伸ばして展示すること自体に新鮮味はないが、バーチャルスライドのタイリング画像であれば、相当引き伸ばしでも十分観察に耐えうることを確認できた点は有用であった。

検討3におけるモバイルパソコンの持ち歩きは、すべての閲覧者が可能な状況とは思われず、可能であれば避けたい動作である。既に述べたように、バーコードリーダーを使う展示標本の配置に関する工夫も必要であろう。他に、この方式に期待できることとして、有機的なファイリングシステムの構築が挙げられる。すなわち、バーコードを介して、ストックしておけば、症例ごとに画像・マクロ像・顕微鏡画像までを直ちに連動させて観察することが可能となる。また実物の臓器以外は、デジタル化しておけば永久に保存が可能である。

E.結論

バーチャルスライドの利用によって、医学部・医学教育博物館において以下のようなシステムを構築することができた。

1）バーチャルスライドシステムを用いた顕微鏡実習用のライブラリ構築によって、同一画像による一斉指導、学生の自己学習が可能となった。

2）バーチャルスライドから取り込んだ顕微鏡画像の大判出力を展示することにより、顕微鏡操作と同等の観察効果が得られることが明らかになった。

3）肉眼臓器にバーコードを貼付けて、バーコードリーダーを接続したパソコンでスキャンすることによって、バーチャル顕微鏡画像の詳細なデータや解説を直ちに見て学ぶことができた。

F.健康危険情報

該当する事項なし

G.研究発表

1. 論文発表

森谷卓也, 中村信彦, 鐵原恵子, 寺岡和美, 皆木純子, 坂本由美, 竹村由布香, 古川典子, 真鍋克己, 仁科幸子, 植木宏明：医学教育博物館におけるバーチャルスライド利用の意義 「医学博物館におけるバーチャルスライド. 日本遠隔医療学会雑誌 6(1),34-37,2010.

2.学会発表

森谷卓也、中村信彦、鐵原恵子、植木宏明：バーチャルスライドシステムを用いた病理学教育：医学教育博物館における経験. 第99回日本病理学会総会（2010年4月28日、東京）

H.知的財産権の出願・登録状況

1. 特許取得

該当する事項なし

2. 実用新案登録

該当する事項なし

3. その他

特記事項なし